HIGH-ORDER HIGH-RESOLUTION RADON TRANSFORM FOR AVO-PRESERVATION MULTIPLES ATTENUATION

YARU XUE, JITAO MA and XIAOHONG CHEN

China University of Petroleum, State Key Laboratory of Petroleum Resources and Prospecting, Beijing, P.R. China. xueyaru@cup.edu.cn

(Received August 28, 2012; revised version accepted January 20, 2013)

ABSTRACT

Xue, Y., Ma, J. and Chen, X., 2013. High-order high-resolution Radon transform for AVO-preservation multiples attenuation. *Journal of Seismic Exploration*, 22: 93-104.

Multiple attenuation and primary energy preservation are important for seismic data processing. Sparse Radon transform can reduce smearing and separate primaries and multiples quite well. But when the primary amplitude varies abruptly, multiple attenuation by sparse Radon transform will be degraded, and the energy of primaries will be distorted. To remediate this problem, we propose a high-order high-resolution Radon transform. Radon transform only performs summation along linear, parabolic or hyperbolic events. Our method incorporates event summation with orthogonal polynomial transform, and meanwhile obtains the gradient and curvature of events. This information will improve resolution of Radon transform in situations where amplitudes vary abruptly with offsets. The high-order Radon transform takes advantages of Radon transform and orthogonal polynomial transform, which will attenuate multiples while preserving AVO information of seismic data. Synthetic data examples show that high-order Radon transform is successful in multiple attenuation and AVO preservation.

KEY WORDS: sparse Radon transform, high-order Radon transform, AVO, orthogonal polynominal transform, multiple attenuation.

INTRODUCTION

Radon transform is widely used in seismic data processing, especially for multiple attenuation and seismic data reconstruction. For the Radon transform in infinite aperture array, one event can be focused into a point; while in reality, because of the finite aperture, the point will be smearing. The smearing will degrade the resolution and distort primary amplitude (Kabir, 1999). Primary with true amplitude will benefit AVO analysis, stack and other processing procedures. How to keep the true primary amplitude is still an open research problem.

0963-0651/13/$5.00

Radon transform is not an orthogonal transform; it is generally posed as an inversion problem. The damping least-squares method is one of most commonly used inversion method (Hampson, 1986), but its resolution in Radon domain is low, especially for multiples with small moveouts. Thorson and Claerbout (1985) proposed a high-resolution Radon transform based on a maximum a posteriori (MAP) stochastic inversion, and forced a local focus in the velocity space. The method is realized in time domain, and involves the inversion of a large matrix, which limited its application. Yilmaz (1989) inverted the Radon transform in frequency domain using singular value decomposition (SVD). SVD can reduce the rank of equations, improve signal to noise ratio, and reduce the smearing. Sacchi (1995) solved the Radon transform problem by deriving a maximum a posteriori estimator at each frequency based on sparsity constraint. This algorithm forces the velocity parameters to concentrate on their main components. This method can improve the resolution in Radon domain, and compensate for the amplitude outside of original aperture. Since then a lot of improved sparse Radon transform methods have been developed in order to prevent aliasing (Cary, 1998; Herrmann, 2000) and preserve the true amplitude (Herrmann, 1999; Schonewille, 2002). From these methods, we can see that the sparsity criterion is helpful to improve resolution and prevent aliasing. However if the sparsity constraint is too strong, fitting with the original data is degraded, although better resolution is obtained. An extreme example is that one point in Radon domain is mapped into an event with constant amplitude, and its AVO information is lost. There must be a trade-off between AVO preservation and high-resolution. Wang (2011) introduced an AVO-preserving sparse parabolic Radon transform. The method split seismic gathers into two Radon gathers: one is the same as the traditional Radon transform, and the other is the one with AVO signature. The method does Radon transform with AVO information, which makes it better than traditional Radon transform. In this paper we propose a Radon transform method focusing on both resolution enhancement and AVO-preservation.

Generally, AVO can be formulated by an even-order polynomial of offsets (Ursin, 1990). Johansen et al. (1995) tracked AVO with unit orthogonal polynomials and showed that AVO of seismic data may be extracted and described by a unique spectrum of polynomial coefficients. In the polynomial fitting, the first three coefficients can be used to reveal AVO characteristics: the zero-th order coefficient is proportional to the stack, the first order represents the mean gradient, and the second describes AVO curvature. Orthogonal polynomial transform for AVO representation is only valid for flat events. Once the event is not strictly flat, the spectra of orthogonal polynomial are smeared and their physical meaning is lost.

Radon transform indeed superposes a set of constant amplitude events, and smearing appears as soon as AVO exists, but it can discriminate events.

Orthogonal polynomial transform can preserve AVO information only for flat layers. Combining those two can give us a high-order high-resolution Radon transform, which can perform Radon transform while preserving AVO information.

THEORY

In this part, we first give a review on the orthogonal polynomial transform, and then we will derive the high-order high-resolution Radon transform.

Orthogonal polynomial transform

It is well known that AVO curve at each sample time t can be represented with even-order polynomials (Ursin and Dahl, 1990), i.e.,

$$d(t,x) = c_0(t) + c_1(t)x^2 + c_2(t)x^4 + \dots \quad , \tag{1}$$

where x and d(t,x) are the offsets and amplitude, respectively, and the $c_j(t)$ are the polynomial coefficients. Note that the $c_j(t)$ coefficients need to be computed jointly. If the fitting order is changed, all of coefficients have to be recalculated.

The orthogonal polynomial transform was introduced by Johansen et al. in 1995, and this transform fits the AVO as follows:

$$d(t,x) = \sum_{j=0}^{M} c_j(t)p_j(x) \quad , \tag{2}$$

where $\{p_j(x), j = 0,1,\dots,M\}$ are a set of unit orthogonal polynomials from offset coordinate x with N+1 samples, M+1 is the number of basis function $p_j(x)$ and each basis function $p_j(x)$ has the general form of a polynomial of degree j. Using the least-squares method, the coefficients can be obtained readily

$$c_j(t) = \sum_{i=0}^{N} d(t,x_i)p_j(x_i) \quad . \tag{3}$$

$c_j(t)$ indicates the j-th order property of AVO at time t. They construct the spectrum of orthogonal polynomial transform. The research of Johansen et al. (1995) showed that this spectrum can be classified as AVO, and this AVO can be represented with the first several orthogonal polynomial coefficients.

In the Appendix, the construction of the orthogonal polynomials is given; it results in a zero-th order polynomial $p_0(x) = 1/\sqrt{(N + 1)}$. In eq. (3), when $j = 0$, the zero-th order orthogonal polynomial coefficients are obtained

$$c_0(t) = [1/\sqrt{(N + 1)}] \sum_{i=0}^{N} d(t,x_i) \quad . \tag{4}$$

It is proportional to stack; on the other hand it is also the Radon transform along the horizontal direction. The first-order coefficient $c_1(t)$ gives the mean gradient of amplitude variations and the second-order coefficient $c_2(t)$ indicates whether the AVO is changing from increasing to decreasing, or vice versa.

We also mention here that the power of the seismic data at time t can also be expressed by orthogonal polynomial coefficients as follows:

$$\sum_{i=0}^{N} d^2(t,x_i) = \sum_{j=0}^{M} c_j^2(t) \quad . \tag{5}$$

High-order Radon transform

Radon transform can be classified into linear, parabolic, and hyperbolic radon transform. Here only the high-order parabolic Radon transform model is given and linear and hyperbolic cases can be obtained in a similar manner.

The parabolic Radon transform performs the amplitude summation along parabolas, as described by the following:

$$m(\tau,q) = \sum_{i=0}^{N} d(t = \tau + qx_i^2,x_i) \quad . \tag{6}$$

It is comparable to the concept of stack with different curvatures. If $q=0$, eq. (6) is proportional to eq. (4). So the Radon transform at $q = 0$ just is the zero-th order orthogonal polynomial transform. Instinctively we hope to get AVO higher order orthogonal polynomial properties along different curvature parabola traces. Thus combining eqs. (3) and (6), we get:

$$m_j(\tau,q) = \sum_{i=0}^{N} d(t = \tau + qx_i^2,x_i)p_j(x_i) \quad . \tag{7}$$

The above transform has the data along the parabolic parameter q at intercept time τ decomposed on every basis function $P_j(x)$. It splits $t-x$ data into high-order Radon domains. The zero-th order Radon profile $m_0(\tau,q)$ is proportional to the traditional Radon transform, with only a scale difference; the first order profile $m_1(\tau,q)$ is a mean gradient gather and it captures the increasing or decreasing trend of amplitude variation with offsets at different direction; the second order $m_2(\tau,q)$ is a curvature gather and describes amplitude increase and then decrease, or vice versa. These first three gathers take most of the energy of the event and are important to get AVO inversion parameters. The other higher order gathers hold information about amplitude detail or noise, and muting them improves the S/N ratio (Johansen et al., 1995).

As $\{p_j(x), j = 0,1,\ldots,M\}$ is a set of unit orthogonal polynomial, it is easy to get inverse high-order Radon transform from eq. (7)

$$d(t,x) = \sum_q \sum_j m_j(\tau = t - qx^2,q)p_j(x) \quad . \tag{8}$$

Obviously the high-order Radon transform simulates events with a linear superposition of a set of orthogonal polynomials, weighted by their Radon gathers respectively. Compared to the traditional Radon transform, the high-order Radon transform includes more amplitude variation information, such as gradient and curvature, besides the stack property.

High-order high-resolution Radon transform

The physical meaning of high-order Radon transform is clear, and it is a highly underdetermined problem because the number of unknown parameters is much larger than the number of knows. In our paper we only consider the three-order Radon transform; they are also important AVO inversion parameters.

Considering the first three orthogonal polynomial transform gathers, eq. (8) can be expressed in the generic matrix form

$$d = \sum_q m_0(\tau = t - qx^2,q)p_0(x) + \sum_j m_1(\tau = t - qx^2,q)p_1(x)$$

$$+ \sum_q m_2(\tau = t - qx^2,q)p_2(x) = (L_0\ L_1\ L_2)\begin{pmatrix} m_0 \\ m_1 \\ m_2 \end{pmatrix} = \mathbf{Lm} \quad , \tag{9}$$

where L_0, L_1, L_2 are the summation operators (the same as L in traditional Radon transform, except for a scale), the gradient operator and curvature operator, respectively. Compared with the traditional Radon transform, eq. (9) is an extended Radon transform with more unknowns because more amplitude variation is included.

To solve the above equation, the sparse inversion method is preferred (Sacchi and Ulrych, 1995; Trad et al., 2003). We need to find optimal Radon gathers by minimizing the following cost function (Trad et. al, 2003)

$$J(m) = \|d - \mathbf{Lm}\|_2^2 + \lambda \|m\|_1^1 \ , \tag{10}$$

where the l_1-norm for the model is chosen in order not to penalize strong large elements contained in the models. The trade-off parameter is used to balance the data fit versus sparsity in high-order Radon domain. The l_1-norm can be transformed to l_2-norm by using model weight matrices, which are proportional to

$$[W_m]_{ii} = 1/\sqrt{|m_i|} \ . \tag{11}$$

Thus

$$\|m\|_1^1 = \sum_i |m_i| = m^T W_m^T W_m m = \|W_m m\|_2^2 \ . \tag{12}$$

It plays a fundamental role in the inversion of sparse models. Using the Iterative Reweighed Least Squares method, at each iteration, only large powers, $|m_i|^2$, are kept, reducing the powers that are not relevant in fitting the data.

In our method Radon panels are composed of three sub-panels, summation panel, gradient panel and curvature panel. For any event, the powers of three panels are different because of AVO property. The model weight matrix of eq. (11) will result in different level sparse constraint for the same event, which distorts the relationship of sub-panel. To overcome this problem, an identical weight matrix is adopted for all sub-panels in order to keep balance between them. Here we utilize the energy distribution of Radon gather. From formula (5), we can obtain the data energy distribution $E(\tau,q)$ in the Radon domain by

$$E(\tau,q) = \sum_{j=0}^{2} m_j^2(\tau,q) \ . \tag{13}$$

And the model weight matrix W_m is proportional to

$$[W_m]_{ii} = 1/\sqrt{E_i} \ . \tag{14}$$

The expression $E(\tau,q)$ describes the energy distribution along different traces at intercept τ, which can capture the main model parameters more precisely than traditional Radon transform m. For example, if event amplitude varies with offset and average is nearly zero, its Radon parameter is also almost zero while it energy is large, which gives more precise sparsity constraint in the Radon domain.

When replicating the above weight vector in diagonal, we get the key inversion weight matrix of high-order Radon transform. Using Iterative Reweighed Least Squares, high-order high-resolution Radon transform is achieved.

EXAMPLES

High-order high-resolution Radon transform combines the Radon transform and an orthogonal polynomial transform. The advantage of this method is AVO-preservation and high-resolution. Here two synthetic examples are given to demonstrate the performance of the proposed method for multiple attenuation and AVO preservation. Firstly, we compare the demultiple ability of the proposed high-order high-resolution Radon transform with high-resolution Radon transform. A CMP gather is displayed in Fig. 1(a). In the figure the amplitude of the primary initially decreases but finally increases with offset, and the amplitude of multiples increases with offsets, which distorts primary. The curve of primary and multiple are shown in Fig. 1(b), and the spectrum calculated by the orthogonal polynomial transform is shown in Fig. 1(c). Fig. 1(c) show that the first three orthogonal polynomial coefficients are enough to represent the AVO curve. From these coefficients, we could estimate the model weight of primary at q = 0. For our method, the model weight is the sum of squared polynomial coefficients, here about 0.97 for three sub-gathers; while for high-resolution Radon transform the model weight is summation of primary amplitude, which is almost zero here, so the focus of high-resolution will be poorer than that of high-order high-resolution Radon transform. The results of

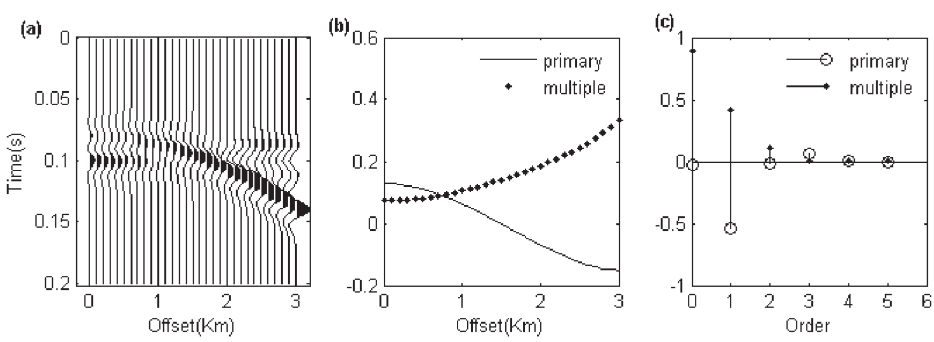

Fig. 1. (a) A synthetic CMP gather with two events with AVO. (b) Curves of primary and multiple. (c) Spectrum of orthogonal polynomial transform for primary and multiple curves.

high-order high-resolution Radon transform are shown in Fig. 2 (a), (b) and (c), the primary and multiple are clearly separated, while the high-resolution Radon transform of primary and multiple, in Fig. 2(d), overlap because of the variations of amplitude, this is consistent with our above analysis. The results of multiple attenuation by muting the parameter $q > 0.01$ s are shown in Figs. 2(e) and 2(f), respectively. The high-order high-resolution method captures variations well while the amplitude of primary using high-resolution Radon transform is distorted. Estimated multiples are also displayed in Fig. 2(g) and (h). The primary residual is obvious with the high-resolution method and the high-order high-resolution Radon transform shows little residuals. This comparison shows that AVO-preserving and resolution of the high-order high-resolution Radon transform outperforms that of the high-resolution Radon transform.

The parameters around $q = 0$ of the three sub-panel of the high-order high-resolution Radon transform ,shown in Fig. 2(a), (b) and (c), match primary orthogonal polynomial coefficients quite well, these primary amplitude variations are the main information needed for AVO inversion. With the proposed method we estimated the zero offset R_0 and gradient G of the primary by removing the first five traces. We evaluated multiple attenuation for different $\Delta\tau_0$ and $\Delta\tau_{max}$, and $\Delta\tau_0$ is the travel time difference between primary and interfering multiple at the minimum offset, and $\Delta\tau_{max}$ the difference at maximum offset. The relative errors (RE) of R_0 and G are computed by the following equation:

$$RE_{\overline{R_0}} = (R_0^{true} - \hat{R})/R_0^{true} \quad , \quad RE_G = (G^{true} - \hat{G})/G^{true} \quad .$$

Fig. 3 shows the results for $\Delta\tau_0 = 0.04$ s and $\Delta\tau_0 = 0.02$ s. It demonstrates the benefit of the proposed method over high-resolution Radon transform. When $\Delta\tau_0$ decreases, the proposed method preserves the relative error to a similar level, whereas the high-resolution Radon transform shows a slightly increasing trend. For the estimation of G, although the result of our method shows more advantage than high-resolution RT, we have to admit that the relative errors clearly increase with $\Delta\tau_0$ decreasing.

We also applied our method on a CMP gather of a Pluto dataset in the left of Fig. 4, most events show amplitude variation with offsets. The primary results are estimated by subtracting the multiple from original gather, shown in the middle and right of Fig. 4 with high-resolution Radon transform and high-order high-resolution Radon transform respectively. Results show that high-resolution Radon transform has multiple residuals left (black arrow), while high-order high-resolution Radon transform can attenuate multiples completely. Primaries obtained by high-order high-resolution Radon transform, pointed by the blue arrow, are much clearer than that of high-resolution Radon transform.

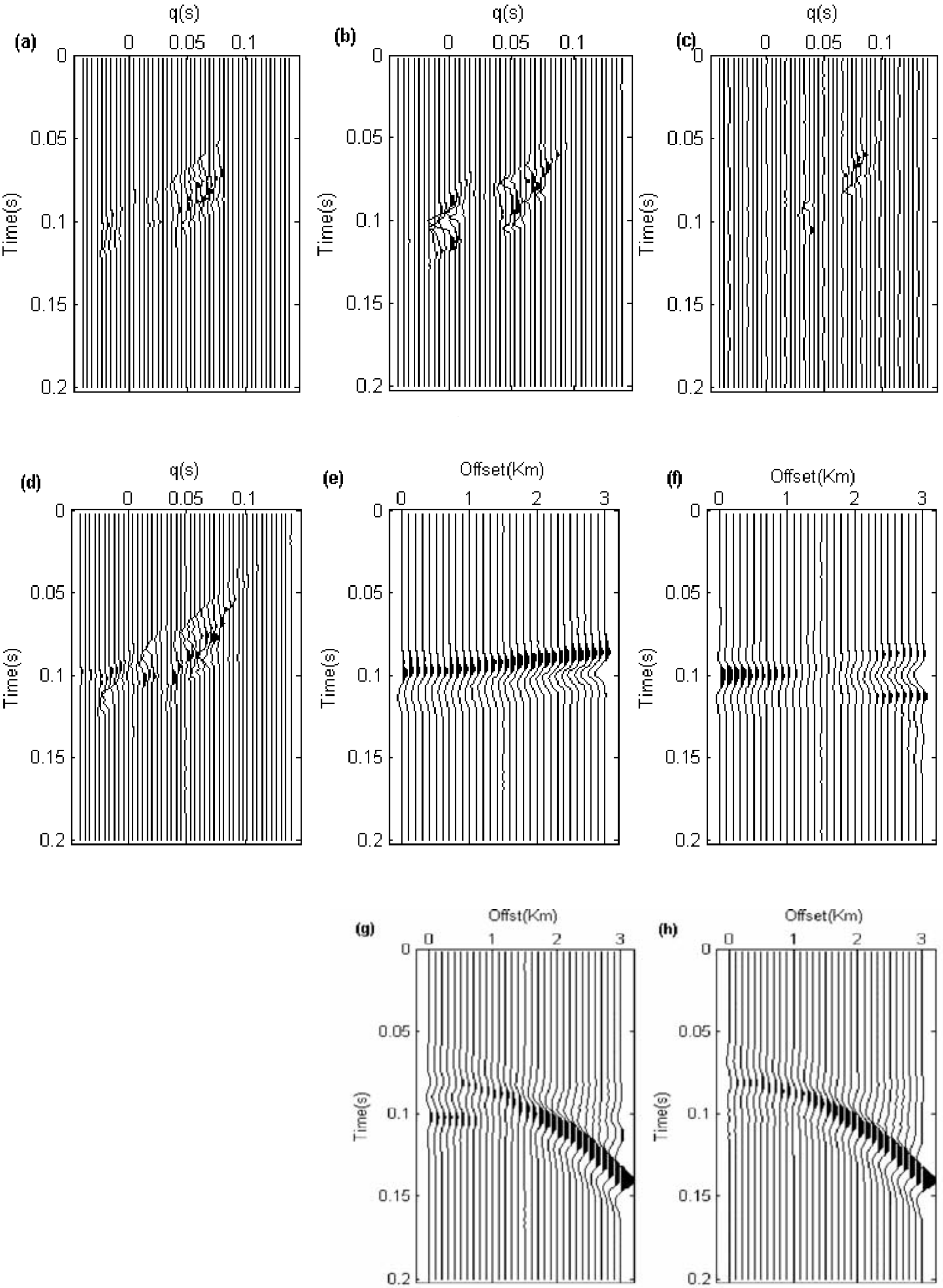

Fig. 2. Demultiple comparison between high-resolution Radon transform and high-order high-resolution Radon transform. (a), (b) and (c) are high-order high-resolution Radon gathers m_0, m_1, m_2, respectively. (d) High-resolution Radon transform gather. Demultiple result of high-resolution Radon transform and high-order high-resolution Radon transform are shown in (e) and (f), respectively. (g) and (h) are estimated multiples with high-resolution Radon transform and high-order high-resolution Radon transform, respectively.

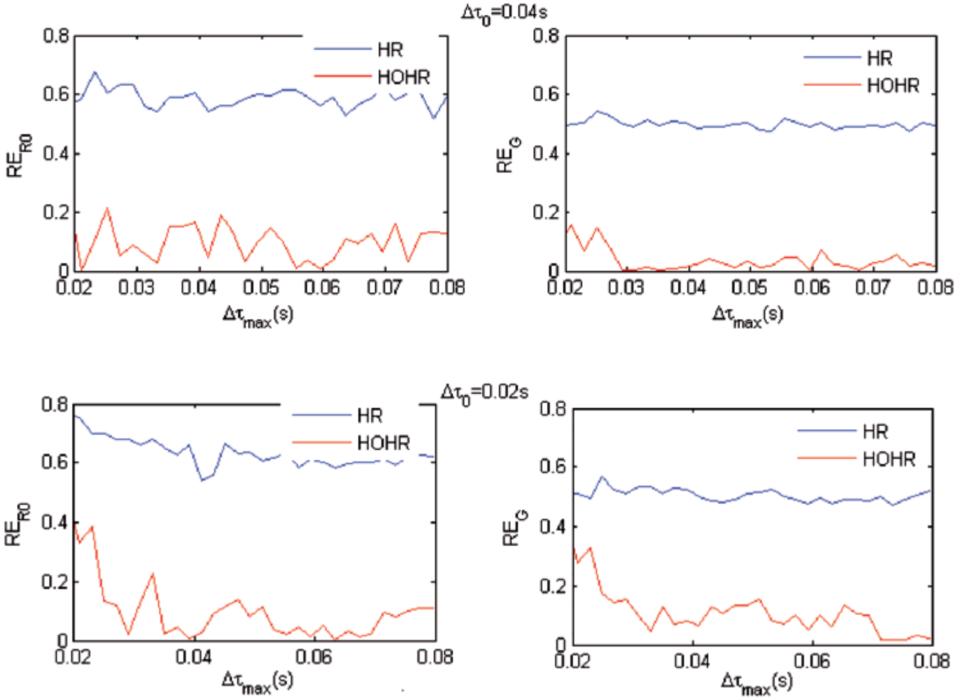

Fig. 3. The relative error of estimated R_0 and G. Top: $\Delta\tau_0$ = 0.04 s. Bottom: $\Delta\tau_0$ = 0.02 s.

CONCLUSION

Multiple elimination and AVO-preservation can benefit seismic data interpretation. Sparse Radon transform improved resolution compared with the traditional Radon transform. We proposed a high-order high-resolution Radon transform method based on Sparse Radon transform and orthogonal polynomial transform. This method extends the Radon transform to three dimensions and gets more information about event amplitude variation with offsets, so it can better preserve the amplitude. But computation cost is an important problem in our method.

Orthogonal polynomial transform is orthogonal and it can represent amplitude completely, so in high-order high-resolution Radon transform any event can be characterized by its curvature parameter and spectrum of orthogonal polynomial transform. Upon this analysis, curvature sample need not satisfy sampling theory and extracting main curvature parameters is sufficient. Thus the inversion space is reduced. This research aspect is left for future work.

Finally, the proposed method can also be applied on data reconstruction and other datasets such as VSP.

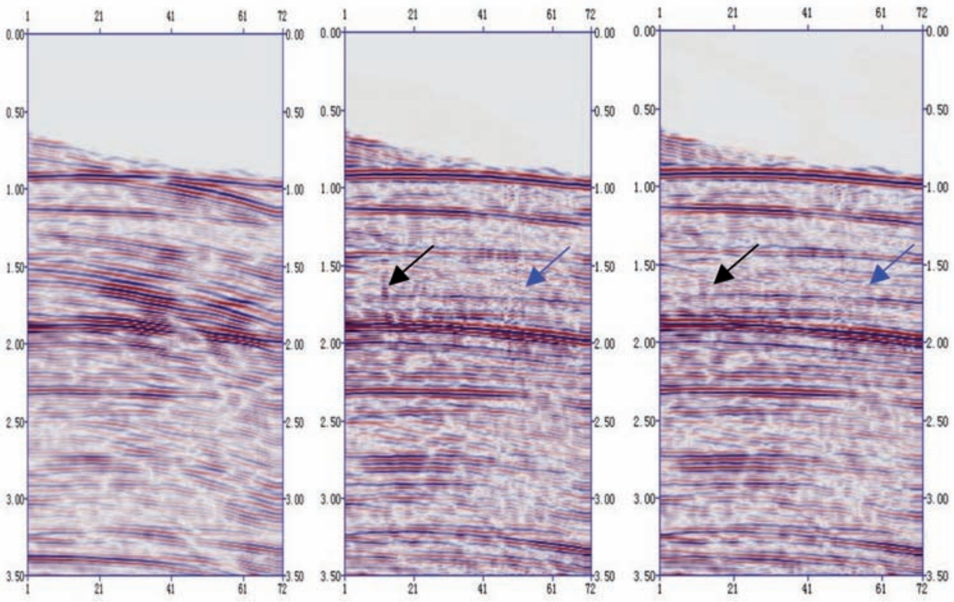

Fig. 4. Demultiple result for a CMP gather of PLUTO data. Left: original data. Middle: demultiple with high-resolution Radon transform. Right: demultiple with high-order high-resolution Radon transform.

ACKNOWLEDGMENTS

This work is partially sponsored by National Natural Science Foundation of China (No. 41004056 and No.41204095) and basic subject fund of China university of Petroleum (Beijing) (JCXK-2011-08). The authors thank Mauricio Sacchi for constructive discussions and useful high-resolution Radon transform codes.

REFERENCES

Cary, P., 1998. The simplest discrete Radon transform. Expanded Abstr., 68th Ann. Internat. SEG Mtg., New Orleans: 1999-2002.

Hampson, D., 1986. Inverse velocity stacking for multiple elimination. J. CSEG, 26: 44-55.

Herrmann, P., Mojesky, T. and Magesan, M., 1999. Amplitude preserving Radon demultiple. Beyond sampling and aperture limitations. Abstracts, Nation. Conv. CSEG: 73-74.

Herrmann, P., Mojesky, T. and Magesan, M., 2000. De-aliased, high-resolution Radon transforms. Expanded Abstr., 70th Ann. Internat. SEG Mtg., Calgary, Alberta: 1953-1956.

Johansen, T.A., Bruland, L. and Lutro, J., 1995. Tracking the amplitude versus offset by using orthogonal polynomials. Geophys. Prosp., 43: 245-261.

Kabir, M.M.N. and Marfurt, K.J., 1999. Toward true amplitude multiple removal. The Leading Edge, 18: 66-73.

Sacchi, M. and Ulrych, T.J,, 1995. High-resolution velocity gathers and offset space reconstruction. Geophysics, 60: 1169-1177.

Schonewille, M., 2002. High-resolution transforms and amplitude preservation. Expanded Abstr., 72th Ann. Internat. SEG Mtg., Salt Lake City: 2066-2069.

Thorson, J.R. and Claerbout, J.F., 1985. Velocity-stack and slant-stack stochastic inversion. Geophysics, 50: 2727-2741.

Trade, D., Ulrich, T.J. and Sacchi, M., 2003. The latest view of sparse Radon transform. Geophysics, 68: 386-399.

Ursin, B. and Dahl, T., 1990. Least-square estimation of reflectivity polynomials. Expanded Abstr., 60th Ann. Internat. SEG Mtg., San Francisco: 1069-1071.

Wang, B., 2011. AVO-preserving sparse parabolic Radon transform. Extended Abstr., 73rd EAGE Conf., Vienna.

Yilmaz, O., 1989. Velocity-stack processing. Geophys. Prosp., 37: 357-382.

APPENDIX

CONSTRUCTION OF ORTHOGONAL POLYNOMIALS

We show how to construct a set of orthogonal polynomials from the offset coordinates x. Let $\{p_0(x), p_1(x), \ldots p_M(x)\}$ be a set of unit orthogonal polynomials, then x^j can be expressed by a linear combination of these basis functions by

$$x^j = \sum_{k=0}^{j} \alpha_{jk} p_k(x) \quad . \tag{A-1}$$

The basis function of polynomial degree j can also be composed by basis functions with degree lower than j, i.e.,

$$P_j(x) = \{x^j - \sum_{k=0}^{j-1} \alpha_{jk} p_k(x)\}/\alpha_{jj} \quad . \tag{A-2}$$

By squaring (A-1) and taking the sum over x, the coefficients α_{jk} are given by

$$\alpha^{jj} = \sum_{i=0}^{N} x_i^j P_j(x_i) \quad , \tag{A-3}$$

and

$$\alpha^{jk} = \sqrt{\{ \sum_{i=0}^{N} (x_i^j)^2 - \sum_{k=0}^{j-1} (\alpha^{jk})^2 \}} \quad , \tag{A-4}$$

A set of orthogonal polynomial from offsets can be constructed based on formulae (A-2)$-$(A-4). First we compute α_{00} from (A-3), and get $\alpha_{00} = \sqrt{(N+1)}$, then $P_0 = 1/\sqrt{(N+1)}$. The subsequent coefficients and polynomials are computed in the following order: α_{10}, α_{11}, P_1, α_{20}, α_{21}, α_{22}, P_2, ... until the order we need.